

The Virtual Screening and Molecular Docking Study of New Inhibitors for SARS-COV-2 Papain-Like Protease (PL^{pro})

Alev ARSLANTÜRK BİNGUL ¹

BİNGUL ¹
Necmettin PİRİNCCİOGLU ²



¹Department of Chemistry, Institute of Natural and Applied Sciences, Dicle University, Diyarbakır, Türkiye

²Department of Chemistry, Dicle University, Faculty of Science, Diyarbakır, Türkiye



 Geliş Tarihi/Received
 21.03.2025

 Kabul Tarihi/Accepted
 03.05.2025

 Yayın Tarihi/Publication
 21.05.2025

 Date

Sorumlu Yazar/Corresponding author: *Necmettin PiRiNCCIOĞLU*,

E-mail: pirincn@dicle.edu.tr

Cite this article: Arslantürk Bingül A, Pirinccioğlu N. The virtual screening and molecular docking study of new inhibitors for SARS-COV-2 papain-like protease (PL^{pro}). *J Ata-Chem*. 2025;5(1): 28-37.



Content of this journal is licensed under a Creative Commons Attribution-Noncommercial 4.0 International License.

SARS-COV-2 Papain Benzeri Proteaz (PLpro) İçin Yeni İnhibitörlerin Sanal Tarama ve Moleküler Yerleştirme Çalışması

ABSTRACT

Although global human mobility has normalized after the COVID-19 pandemic, the disease remains a major threat due to the emergence of new variants, keeping it a key target for drug development. Considerable efforts have been put to understand the disease, to create treatment options, and ultimately to eradicate it. It has been shown that these viruses have the largest genome size among all known RNA viruses, with their genome consisting of an RNA strand enclosed in a protein coat. PL^{pro} is an enzymatic protein which is necessary for the replication process of SARS-CoV-2 and during viral infection, it is essential in helping coronaviruses evade the host's innate immune defense. Consequently, targeting PL^{pro} in antiviral drug development could be an effective approach to inhibit viral replication and interfere with signaling pathways in infected cells. This study aims to provide new potential inhibitor candidates for PL^{pro} (PDB: 7LOS) by molecular modelling study. A total of over 2 million molecules from ZINC15 database have been screened against PL^{pro} by structure- based virtual screening, followed by molecular docking. The docking scores of the top five ligands were in the range of -81.57 kcal/mol and -83.19 kcal/mol, which were much better than that of co-crystallized ligand Y97 (-58.25 kcal/mol). The docking results indicated that ligands interact with the key residues (Asp 164, Arg 166, and Glu167) in the active pocket of PL^{pro}. H02 revealed some physicochemical properties as a potential hit according to the ADME results.

Keywords: SARS-CoV-2, PL^{pro} inhibitors, virtual screening, molecular docking, drug design

ÖZ

COVID-19 salgını sonrasında küresel insan hareketliliği normale dönmüş olsa da, hastalık yeni varyantların ortaya çıkması nedeniyle büyük bir tehdit olmaya devam ediyor. Bu sebeple, hastalığı anlamak, tedavi seçenekleri oluşturmak ve nihayetinde ortadan kaldırmak için önemli çabalar sarf edilmektedir. Bu virüslerin, bilinen tüm RNA virüsleri arasında en büyük genom boyutuna sahip olduğu ve genomlarının bir protein kılıfı içinde bulunan bir RNA ipliğinden oluştuğu kanıtlanmıştır. PLpro, SARS-CoV-2'nin replikasyon süreci için gerekli olan enzimatik bir proteinidir ve viral enfeksiyon sırasında koronavirüslerin konağın doğuştan gelen bağışıklık savunmasından kaçmasına yardımcı olmakta görevlidir. Sonuç olarak, antiviral ilaç geliştirmede PLpro'yu hedeflemek, viral replikasyonu inhibe etmek ve enfekte hücrelerdeki sinyal yollarına müdahale etmek için etkili bir yaklaşım olabilir. Bu çalışma, moleküler modelleme çalışmasıyla PLpro (PDB: 7LOS) için yeni potansiyel inhibitör adayları sağlamayı amaçlamaktadır. ZINC15 veritabanından 2 milyondan fazla molekül, yapı tabanlı sanal tarama ve ardından moleküler yerleştirme ile PLpro'ya karşı tarandı. İlk beş ligandın yerleştirme puanları, eş-kristalize ligand Y97'nin (-58,25 kcal/mol) puanlarından çok daha iyi olan -81,57 kcal/mol ve -83,19 kcal/mol aralığındaydı. Yerleştirme sonuçları, ligandların PLpro'nun aktif cebindeki anahtar kalıntılarla (Asp 164, Arg 166 ve Glu167) etkileşime girdiğini gösterdi. ADME sonuçlarına göre H02, potansiyel bir hedef olarak bazı fizikokimyasal özellikler ortaya koydu.

Anahtar Kelimeler: SARS-CoV-2, PL^{pro} inhibitörleri, sanal tarama, moleküler yerleştirme, ilaç tasarımı

INTRODUCTION

Coronavirus disease 2019 (COVID-19) outbreak, known as Wuhan Novel Coronavirus (COVID-19) has raised due to a group of viruses that can affect many animals and cause respiratory infections in humans through transmission.¹⁻⁴ This infection, which spreads rapidly from person to person, has become a major problem for many countries in terms of health and other sociological aspects. 5 Scientists made tremendous efforts to understand the disease, develop treatment methods, and ultimately eliminate the disease entirely. 6,7 An intense work carried out by the biologist has revealed that these viruses have the largest genome size among the known RNA viruses,8 and their genome is composed of an RNA strand surrounded by a protein coat.9 Due to their long RNA genomes, many mutations occur during the copying of genetic material.8 The possible mutations are expected to lead to the emergence of concerning variants. These variants are dangerous for public health and may result in the formation of different strains that could cause future epidemics.

A series of structural proteins, namely nucleocapsid (N), envelope (E), membrane (M), and spike (S), are involved in the virus's mechanism of infecting the host. 10,11 The process begins with the virus binding to the host cell using its surface spike protein (S) to enter the cell through endocytosis. During this process, the angiotensinconverting enzyme 2 (ACE2) receptor on the surface of human cells acts as the target structure for the virus to bind. Once inside the host, the virus releases its singlestranded RNA, which carries its genetic information, allowing this RNA to bind to the host cell's ribosomes. This binding enables the synthesis of several essential enzymatic proteins, including RNA polymerase, the main protease (M^{pro}), and papain-like cysteine protease (PL^{pro}), which are necessary for the replication process for SARS-CoV-2.¹² Consequently, they have been essential targets for antiviral drug development

The critical role of the papain-like protease (PL^{pro}) enzyme in viral replication is due to its function as a cysteine protease. Upon infection, the viral RNA is converted into replicase polyproteins, pp1a and pp1ab. PL^{pro} is involved in the cleavage of non-structural proteins (NSP1-NSP6) from the polyproteins and form replication-transcription complexes. The synthesis of the viral genome and the direction of replication depend on the formation of these complexes.¹³ There are a range of key components of these replication-transcription complexes and NSP3,

including PL^{pro}, plays a role in processing polyproteins and modulating host immune responses.¹⁴

During viral infection, PL^{pro} plays a crucial role in avoiding coronaviruses from the host's innate immune response. PL^{pro} is responsible for removing cellular proteins such as ubiquitin (Ub) and ISG15 (interferoninduced gene, which are involved in initiating the host's innate immune response. Therefore, targeting PL^{pro} in the design of antiviral drugs can be an important strategy to inhibit viral replication and disrupt signaling pathways in infected cells.

The U.S. Food and Drug Administration (FDA) has authorized only a few antiviral drugs for emergency use. Remdesivir (Veklury) and molnupiravir (Lagevrio), although originally developed for other viral infections, have been repurposed for SARS-CoV-2. These drugs work by targeting the viral RNA-dependent RNA polymerase (RdRp) enzyme.¹⁹ Paxlovid, which is used as a combination of two drugs, nirmatrelvir and ritonavir, is another medication for SARS-CoV-2. Nirmatrelvir inhibits the main cysteine protease (Mpro or 3CLpro) of SARS-CoV-2, while ritonavir helps maintain the necessary conditions for nirmatrelvir to reach effective concentrations against SARS-CoV-2.20 Although PL^{pro} is a potential target for SARS-CoV-2 treatment, it has been found that developing effective and applicable inhibitors is challenging. The primary reason for this is the characteristics of the P1 and P2 regions, which do not allow drugs to bind near the cysteine residue in the active site.²¹ Suitable inhibitors for cysteine protease enzymes are identified when the P1 and P2 regions are targeted, and covalent interactions are formed near the cysteine residue in the active site.²² This makes it very difficult to identify new suitable inhibitors for PL^{pro} inhibition and to repurpose existing ones. The drug discovery process was directed to find a new potential target and BL2-groove is now considered as an alternative location of PL^{pro} enzyme.²³⁻²⁵

A range of literature has been reported for the determination of essential roles of PL^{pro}. Dhananjay et al. screened 659 compounds from the NPASS database, and ten compounds were detected as hits and further interaction study was carried out. The compounds demonstrated interactions with the Tyr264, His175, Asp 164, Arg166, Asp302 amino acids residues which are identical with the residues reported in our study.²⁶ Another study²⁷ revealed that the screened compounds showed hydrophobic interactions with the Leu162, Gly163, Met208, Pro247, Pro248, Tyr264, Gly266 and Tyr273, hydrophilic interactions with the polar acceptor residues

Arg166 Gln269 and polar donor residues Asp164, Thr301, Glu161. Most of the reported amino acids were also detected in our study.

In this study, it was aimed to determine compounds as candidate inhibitors for PL^{pro} from the public libraries provided by the repositories ZINC 15 by integrating multiple computational approaches namely molecular docking. The best five results of molecules have been detected with the highest docking scores obtained with molecular docking study compared to the co-crystallized ligand and further evaluation have been proceeded. Screening strategy was designed to start with a compound library of over 2 million compounds from the ZINC 15 library. The library provided a large, well-curated set of commercially available compounds in formats (e.g., mol2 with protonation states and 3D conformations) directly compatible with structure-based virtual screening and DOCK 6 workflows. ZINC15 has been extensively utilized in molecular docking studies, previous enabling reproducibility and facilitating comparison with established literature. The compound repository was narrowed due to the large number of molecules in the ZINC databases to focus on the commercially available targets as well as the chemical fulfilling the druglike and ADME properties. Receptor-based screening was performed in compliance with the better ligand-based screening. The compounds were classified according to the ADME and bioavailability properties obtained from screening.

METHODS

Ligand Library Design

The dockable poses of over 2 million compounds extracted from ZINC15²⁴ database were subjected to the virtual screening using Dock 6.7²⁵ to identify molecules with suitable adaptability to PL^{pro}. They were filtrated as only 3D structures aiming to find as many molecules as possible to search for inhibition effect on main protease. Since the ZINC15 includes mol2 file format of molecules compatible with Dock6, the molecules were ready for molecular docking study.

Molecular Docking

As a target protein, x-ray crystal structure of PL^{pro} (PDB:7LOS)²⁶ was obtained from the Protein Data Bank (http://www.rcsb.). PDB entry 7LOS was selected for docking studies due to its high-resolution structure (2.49 Å) of the SARS-CoV-2 papain-like protease (PLpro) in complex

with a non-covalent inhibitor. This structure was chosen because it provides a well-defined binding site, relevant to our study, with a co-crystallized ligand, allowing for accurate comparison of docking results. The docking procedure consists of four main steps. In the first step, both the ligand and the protein are prepared using UCSF Chimera. Initially, the ligand and other non-standard residues are removed from the protein structure. Subsequently, a molecular surface is generated around the protein (excluding hydrogens) using the DMS (Dot Molecular Surface) algorithm, originally developed by Richards²⁸ and later adapted by Connolly.²⁹ Hydrogen atoms are then added to the receptor, and atomic charges are calculated using Chimera. The resulting file is saved in SYBYL mol2 format. The ligand is extracted as a separate file from the crystal structure (PDB ID: 7SOL), hydrogens are added, and its charges are computed in its ionic form using Chimera. The ligand file is also saved in SYBYL mol2 format, without further energy minimization.

In the second step, receptor-based spheres are generated to define the potential binding site. The program sphgen, as implemented in DOCK³⁰, is used to generate spheres based on the molecular surface and surface normal, using minimum and maximum sphere radii of 1.4 Å and 4.0 Å, respectively. Since the binding site is known, a subset of spheres within a defined radius is selected to represent the active site. The program sphere selector, implemented in DOCK 6, is employed to select all spheres located within 10.0 Å root-mean-square deviation (RMSD) of every atom in the crystallographic ligand structure.

The third step involves the generation of the energy grid. This begins with the creation of a grid box surrounding the selected spheres. The coordinates and dimensions of the box are defined as 3.000, 12.000, and 35.000 Å, with a grid size of $30 \times 30 \times 30$ Å. The grid program, as implemented in DOCK 6, is used to generate scoring grids within the defined binding region.

The final step is flexible docking, where the receptor is treated as a rigid body while the ligand is allowed to explore conformational and orientational flexibility.

Absorption, distribution, metabolism, excretion and toxicity (ADMET) prediction

The ADME properties of ligands by SwissADME web service were also defined to identify the physicochemical and drug likeness properties of the ligands. The level of gastrointestinal absorption, blood-brain barrier (BBB) penetration, bioavailability and inhibition efficiency of a

range of hemeproteins namely, CYP1A2, CYP2C19, CYP2C9, CYP2D6, and CYP3A4 enzymes were identified as physicochemical properties of the compounds.

RESULTS

Molecular Docking Studies

The structures of the co-crystallized ligand (Y97) and hits are shown in Figure 1. The validation of the docking process was tested by re-docking of the co-crystallized ligand to the protein by Dock 6.7. The docked pose of the ligand was compared with its x-ray coordinates having a RMSD of 1.383 Å (Figure 2). The docking pose shows a similar conformational pattern with the co-crystallized ligand. The binding mode of Y97 with the protein is demonstrated in Figure 2.

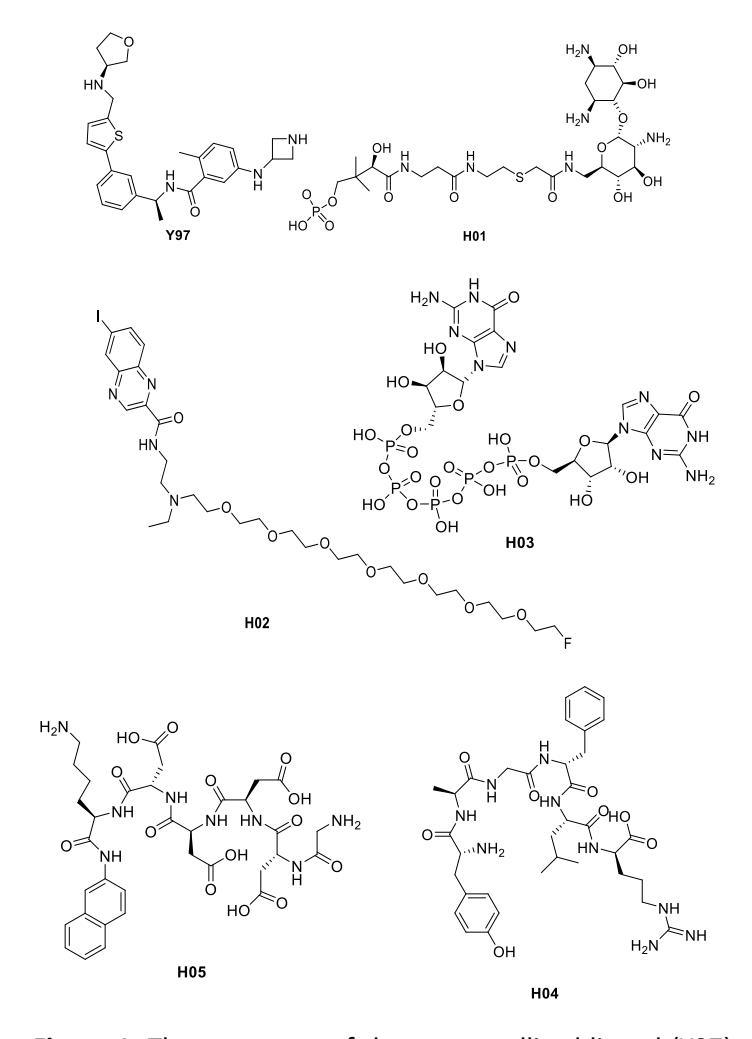


Figure 1. The structures of the co-crystallized ligand (Y97) and hits.

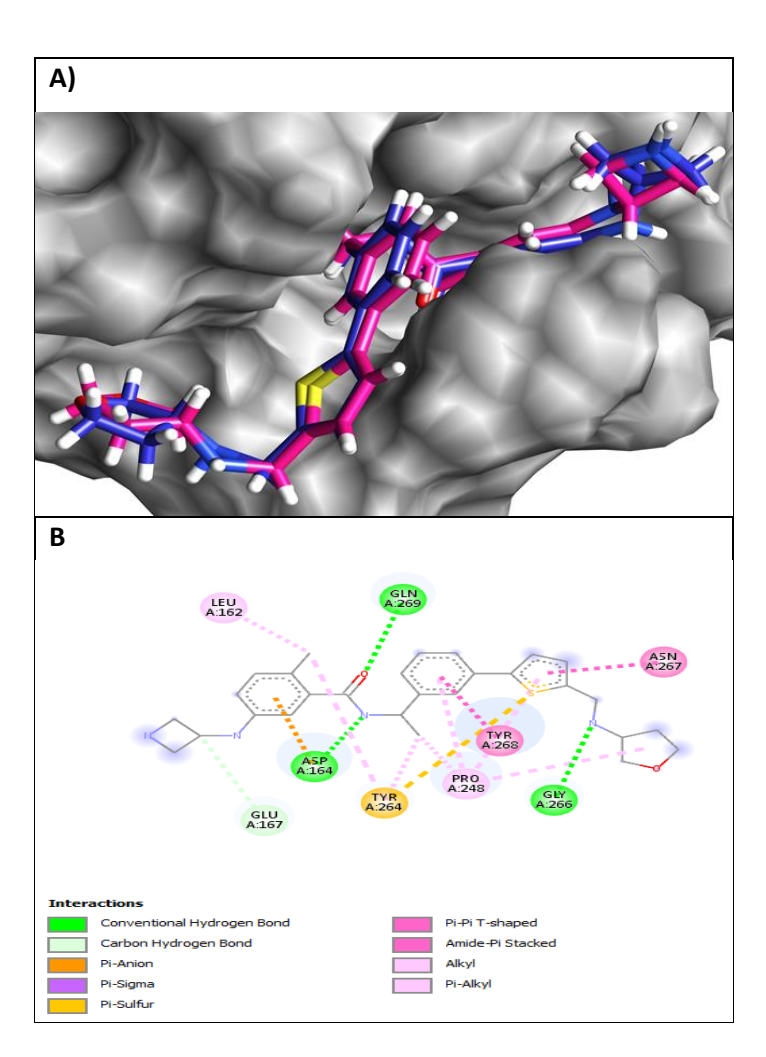


Figure 2. A) The superimposed structure of the cocrystallized ligand (blue) Y97 with the docked pose having a RMSD value of 1.383 Å. B) 2D structure of ligand on catalytic site.

The binding mode of the ligand Y97 involves a range of its interactions with key amino acid residues in the protein. There are diverse interactions, including hydrogen bonds, pi, and hydrophobic interactions. The cyclic amine on the azetidine ring forms a conventional hydrogen bond with Glu167 while the benzene next to the cyclic amine has a pi-sigma and a pi-anion interaction with Asp164. It also interacts with Pro248 via the benzene ring by means of Tshaped pi-alkyl interactions and via the thiophene rings by pi-alkyl interactions. The secondary amine next to the tetrahydrofuran group with interacts with Arg267 through a conventional hydrogen bond and the thiophene ring-with this residue through amide-pi interaction. The amide group also forms a hydrogen bond with Gln 269. Finally, the methyl substitution on the benzene ring interacts with Leu162 via a hydrophobic manner.

Following the validation process, over 2 million compounds were placed into a binding site of PL^{pro}, specifically BL2-groove, molecular docking method. The compounds were sorted according to their docking scores, having the best scores, along with the re-docked cocrystalized ligand were investigated. This study discusses the selected five compounds in terms of having the best docking scores compared to the Y97 ligand and the scores given in Table 1. The scores given in the table are the DOCK 6 scoring function outputs not actual binding free energy. The top five molecules with the highest binding scores were selected for detailed analysis and further in silico evaluations. These compounds, for which the advanced studies (MD simulations and MM-PBSA studies) are ongoing, were chosen to reduce computational costs, limit the number of candidate compounds for experimental validation, and enhance focus by prioritizing the most promising ligands. The information provided in this report is limited to molecular docking results only, as it serves as a preliminary report. According to the results H01 ligand has the best docking score with the value of -83.191 kcal/mol.

Table 1. Scores (DOCK 6 scoring function outputs) of the best five ligands in binding site of PL^{pro} (papain-like protease) obtained from molecular docking studies

_				
Dock Score (kcal/mol)				
-83.191				
-82.422				
-82.347				
-81.709				
-81.574				
-58.246				

DISCUSSION

Docking studies revealed that hit compounds mainly interact with Gly266, Pro299, Pro248, Tyr264, Arg166, Asp164, Gly163, Gln269, Glu167, Tyr268, Leu162, Lys232, Thr302 and Ser160 residues via hydrogen bonds. The individual binding mode of hits with the protein is demonstrated in Figure 3.

A recent study has highlighted several FDA-approved drugs exhibiting strong binding affinities to the BL2 groove of PLpro. Imatinib, commonly used in leukemia treatment, demonstrated a notable binding affinity with a docking score of -11.95 kcal/mol. Simeprevir used as an antiviral

agent for hepatitis C showed a docking score of -11.20 kcal/mol. Two drugs, Naldemedine and Tucatinib, exhibited identical docking scores of -11.07 kcal/mol and Erdafitinib. prescribed for metastatic urothelial carcinoma, presented a docking score of -10.94 kcal/mol. The binding interactions within the BL2 groove are primarily facilitated by specific residues. Tyr 264 and Tyr 268 residues significantly contribute to ligand binding through hydrophobic interactions. Gln 269 is involved in hydrogen bonding, aiding in ligand stabilization.³¹ Another study revealed that Aspergillipeptide F is one of the best potential PL^{pro} inhibitors. with a pharmacophore-fit score of 75.916 kcal/mol.²⁴ Garland et al. reported some non-covalent PLpro inhibitor through a large scale of virtual screening which the ZINC20 library was used as the source of the compound and experimental study is provided. 32 This study detailed interaction maps provides via crystallography and SPR; confirmed key residues such as Tyr268, Asp164. In our study a detailed in-silico binding mode analysis confirms similar key residues. Importantly, none of the molecule was reported in Garland's study which have been identified as the hit in our study Despite the absence of experimental data, our study provides novel contributions to the computational landscape by offering valuable pharmacokinetic profiles. In addition to that, our manuscript explores novel ligand scaffolds derived from available ZINC15 compounds, some of which show structural divergence from the known GRL-0617 analogs used in Garland et al.32

Most interactions for the H01 occur through conventional hydrogen bonds. The amide group on the long chain forms hydrogen bonds via its NH and carbonyl groups with the amino acid residues Asp 164 and Pro 248, respectively. The thioether linkage and the amino hydrogen on the cyclohexane ring interact with Gln 269. Additionally, the NH group on the cyclohexane scaffold forms an extra hydrogen bond with Leu 162, and Glu 161 forms hydrogen bonds with both the hydroxyl group on the cyclohexane ring and the amine group on the pyran ring. The phosphate group interacts with Arg 166, likely forming a salt bridge through a combination of electrostatic attraction and hydrogen bonding. Furthermore, additional carbon-hydrogen bonds are observed with Asp 164, Leu 162, and Glu 161. Hydrogens on the methylene group near the amide and on the carbon bonded to the cyclohexane hydroxyl group also contribute to these interactions.

The interactions for H02 predominantly occur through conventional hydrogen bonds with various amino acid residues. Lys 232, Tyr 207, Arg 166, and Met 206 form

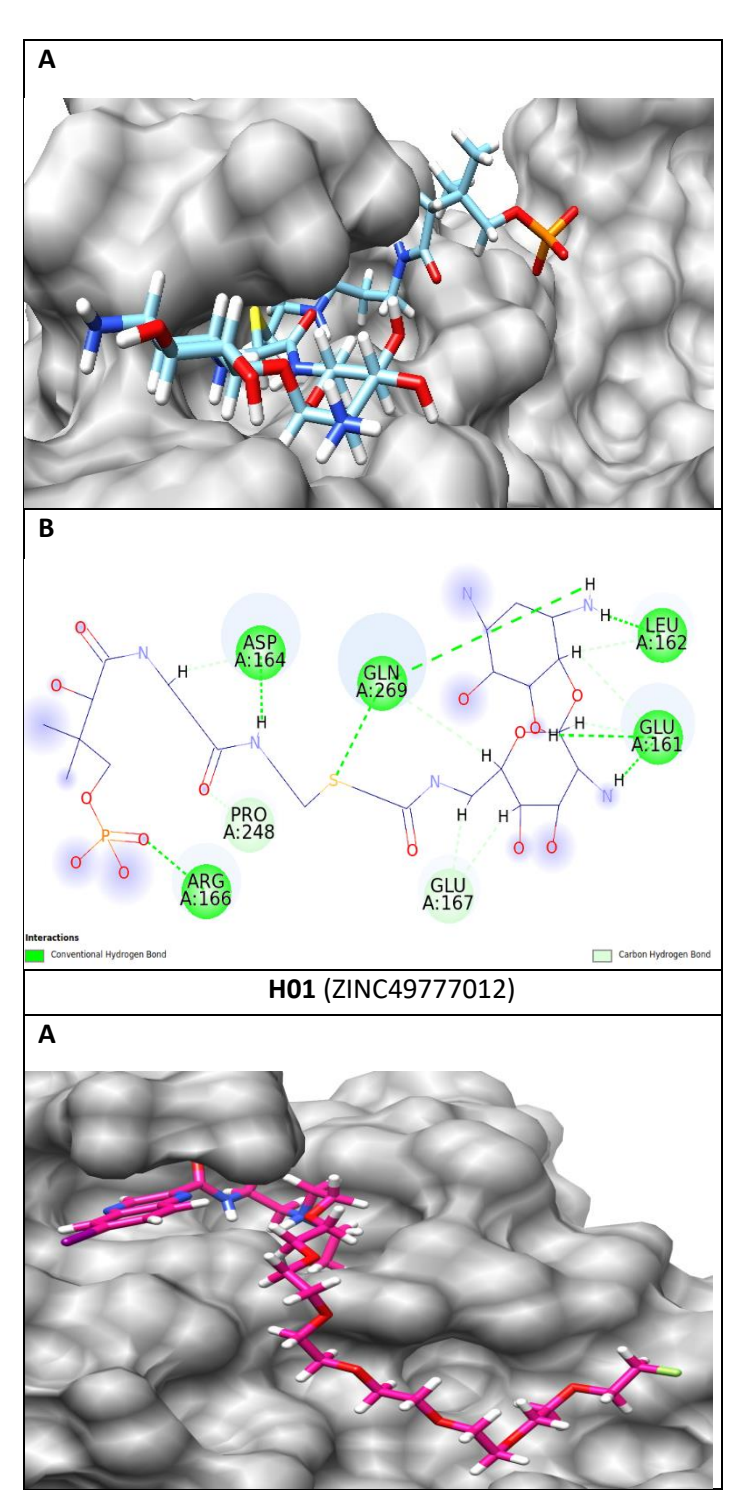
hydrogen bonds with the fluorine and ether functionalities on the polyether chain. Gln 269 establishes a conventional hydrogen bond with the amide carbonyl group near the pyrazine ring. Asp 164 is the residue involved in the most interactions; the tertiary amine nitrogen, the amide nitrogen, and the pyrazine nitrogen all contribute to these interactions. The tertiary amine nitrogen forms a salt bridge with Asp 164, mediated by electrostatic attraction between the positively charged amine group and the negatively charged carboxylate group of Asp 164. Additionally, the pyrazine ring forms a π -anion interaction with Thr 301, and a similar π -anion interaction is observed between the benzene ring attached to the pyrazine and Glu 167.

In the case of H03, the phosphate moiety forms a conventional hydrogen bond exclusively with the Arg 166 residue. It also establishes a salt bridge with Arg 166, involving electrostatic attraction and possibly hydrogen bonding, thereby contributing to the overall stability of the ligand-protein interaction. Carbon-hydrogen bonds involve primarily hydrogen atoms from the tetrahydrofuran ring, which interact with Tyr 268, Glu 167, and Gln 269. Gln 269 engages in a π–sigma interaction with the imidazole ring. The imidazole and pyrimidine rings are responsible for amide π -stacked interactions with Gly 163. Another carbon-hydrogen bond is formed between the pyrimidine NH and Tyr 264. Asp 164 engages in a π-anion interaction with the pyrimidine ring. Pro 299 and Pro 248 contribute π -alkyl interactions with the aromatic imidazole ring. Finally, Glu 266 forms a strong conventional hydrogen bond with the nitrogen atom of the imidazole ring.

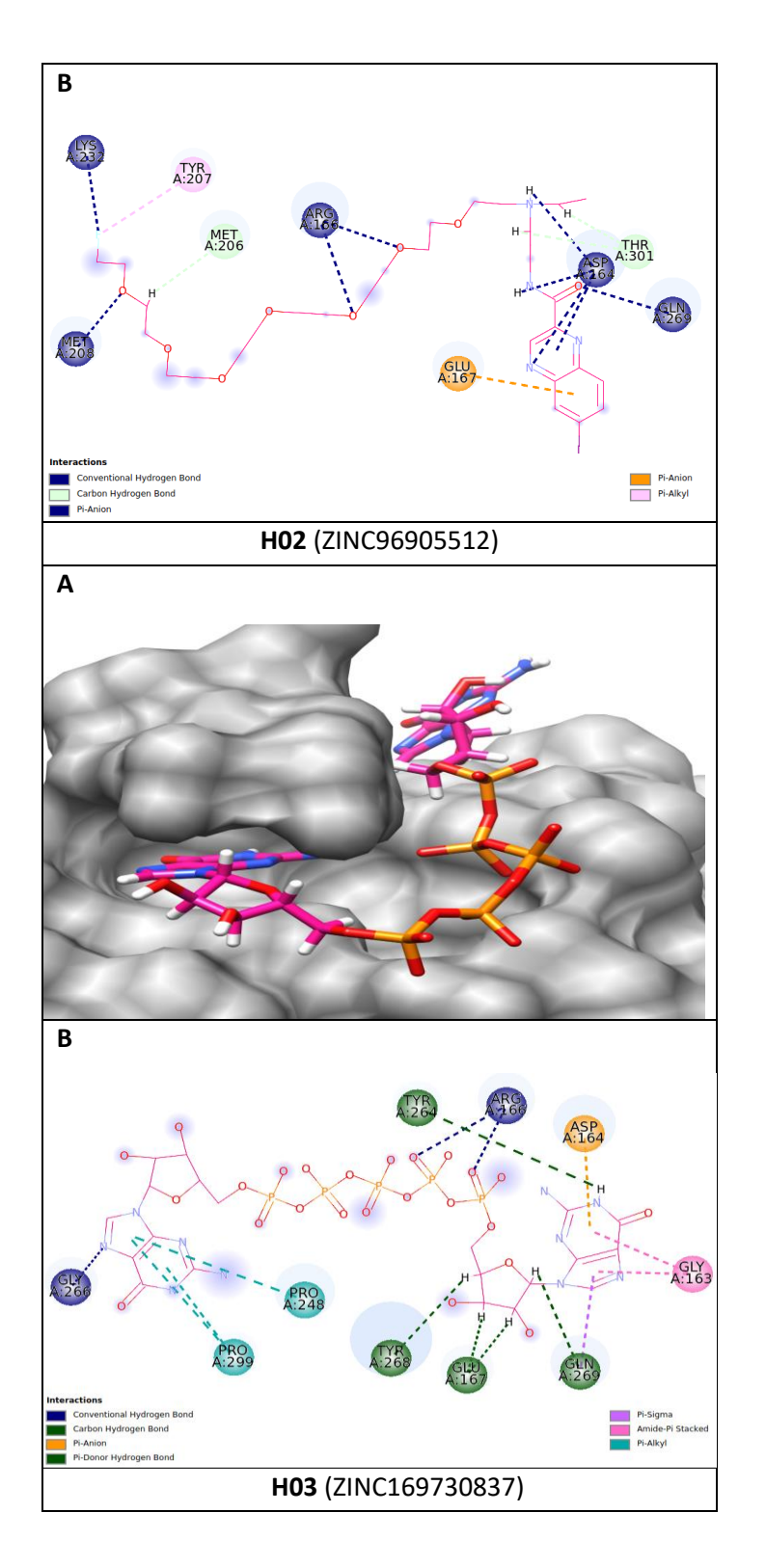
The strongest interactions for H04 occur between the guanidine moiety and the residues Gln 174 and Glu 103. The amide fragment also plays a significant role by forming conventional hydrogen bonds, particularly between the amide carbonyl group and Arg 166. The main salt bridge in this interaction profile is formed between Arg 166 and Glu 103. where electrostatic attraction between the guanidinium group and the carboxylate group contributes to the stability of the ligand-protein complex. Additionally, the amide hydrogen and nearby amino hydrogens form hydrogen bonds with Thr 301 and Tyr 273. Other interactions include a π -alkyl attraction between the isopropyl group and Tyr 171, as well as a carbon-hydrogen bond between the carboxylic acid on the aliphatic linker and Ser 170.

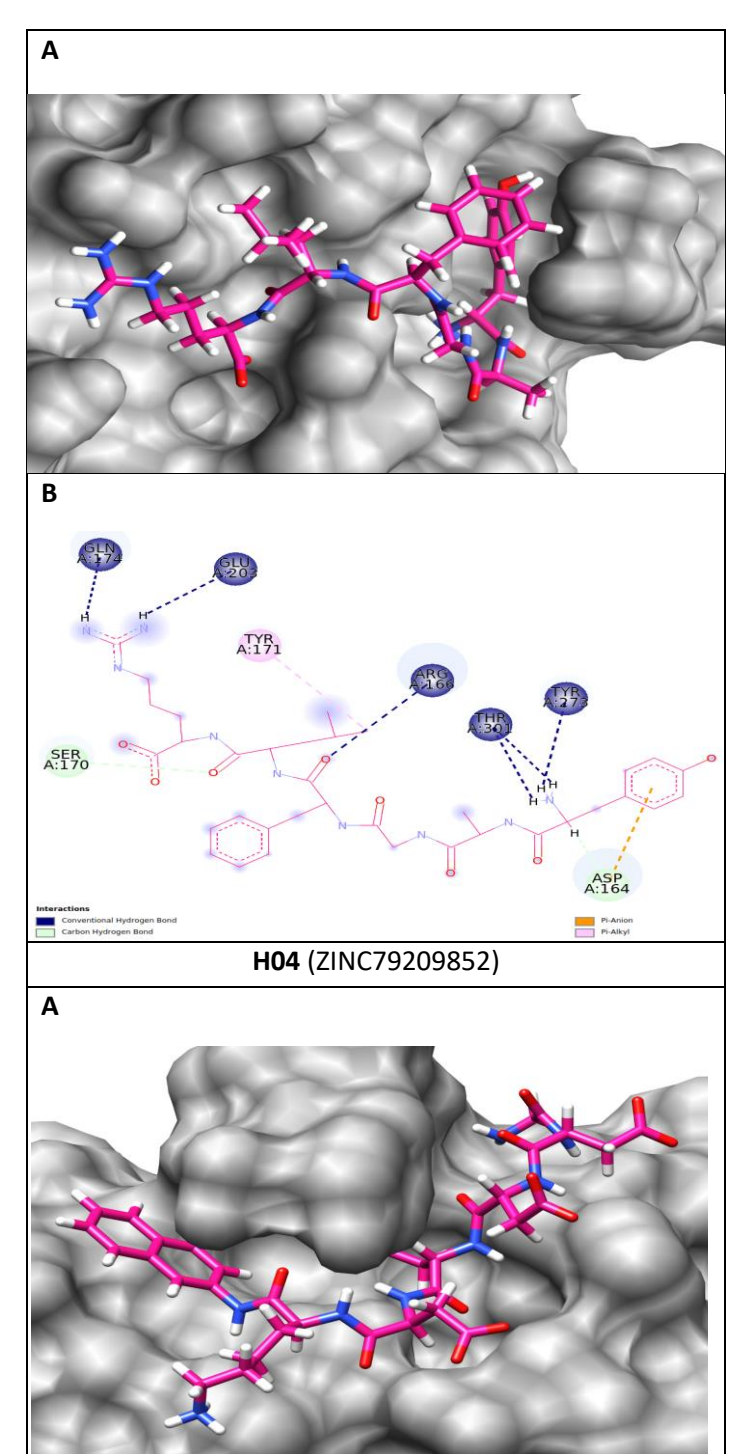
In the case of H05, the amino acid residues primarily interact through conventional hydrogen bonds with the hydrophilic groups of the molecule. The hydrogens of the

amide group form these interactions with Gly 266, Pro 248, Glu 167, and Tyr 268. Additionally, Tyr 268 and Arg 166 establish conventional hydrogen bonds with the amide carbonyl group. Arg 166 also forms a conventional hydrogen bond with the carboxylic acid group, and Tyr 273 participates in this interaction as well. Furthermore, a π -anion interaction occurs between the naphthalene ring and Glu 161, which helps stabilize the overall binding (Figure 3).



J Ata-Chem





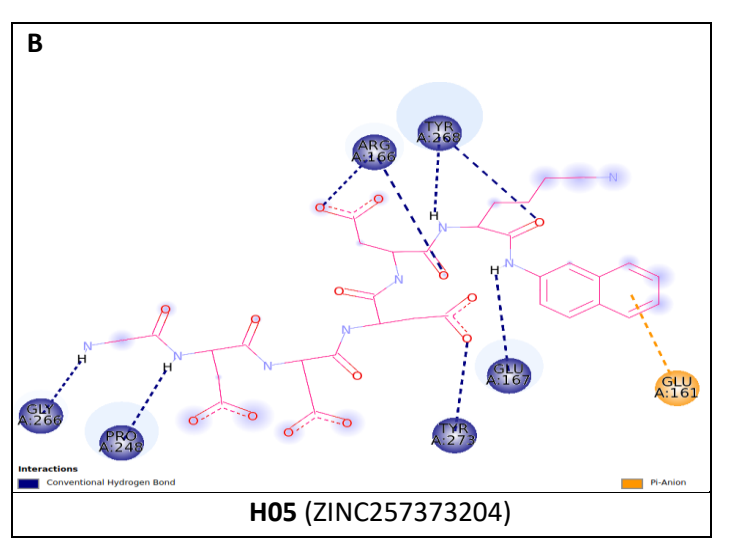


Figure 3. The surface **(A)** and 2D **(B)** structures of the complexes of the ligands with PL^{pro} produced by docking.

ADME results were given Table 2 and 3. According to results, H02 ligand demonstrated high level gastrointestinal absorption property, however none of the ligand showed blood-brain barrier permeation

characteristic (Table 2 and 3). CYP1A2, CYP2C19, CYP2C9, CYP2D6, and CYP3A4 enzymes are different forms of Cytochrome P450 (CYP) protein which are assumed to be crucial for drug metabolism. Analyses revealed that the inhibitory potency of all the ligands was determined at sufficient level toward the CYP1A2, CYP2C19, CYP2C9, CYP2D6, and CYP3A4 enzymes except HIT 02 were found to be effective for the CYP3A4 enzyme inhibition. Bioavailability and molar refractivity results were measured as 0.17 and 167.13, respectively.

Table 2. Physicochemical properties of ligands obtained from SwissADME

Ligand	Molecular mass	H-bond acceptors	H-bond donors	Molar refractivity
H01	720.73	17	13	162.57
H02	724.6	12	1	167.13
H03	948.37	28	13	182.2
H04	725.83	10	11	192.26
H05	788.76	16	12	191.53

Table 3. Predicted ADME properties of the ligands

Ligand	GI	BBB	Bio	CYP1A2	CYP2C19	CYP2C9	CYP2D6	CYP3A4
	absorption	permeant	Availability					
H01	Low	No	0.17	No	No	No	No	No
H02	High	No	0.17	No	No	No	No	Yes
H03	Low	No	0.11	No	No	No	No	No
H04	Low	No	0.17	No	No	No	No	No
H05	Low	No	0.11	No	No	No	No	No

CONCLUSION

Many compounds were screened against PL^{pro} in a hunt to find potential severe acute respiratory syndrome (SARS-CoV)-2 drugs. A total of five hits were found as potential PL^{pro} inhibitors. It was observed that salt bridges are essential for a favorable binding of ligands to the protein. So, H01 with two salt bridges has the highest docking scores. According to the ADME results H02 were found to be a potential candidate in terms of drug-likeness. Molecular dynamic calculations are further needed to evaluate the binding energies of these ligands and consequently their roles in the conformational changes in the active site of the PL^{pro}.

Hakem Değerlendirmesi: Dış bağımsız.

Yazar Katkıları: Necmettin Pirinccioglu: Konsept; Tasarım; Denetim; Kaynaklar; Analiz ve Yorumlama; Eleştirel İnceleme. Alev Arslantürk Bingul: Veri Toplama ve İşleme; Analiz ve Yorumlama; Literatür Taraması; Makale Yazımı.

Teşekkür: Yazar (AAB), Bilim ve Teknolojide Öncelikli Alanlarda 2211-C Ulusal Doktora Bursu Programı başlıklı burs için TÜBİTAK'a teşekkür etmek ister. Yazarlar ayrıca moleküler yerleştirme işlemi sırasında (TRUBA kaynaklarının) kullanımına izin verdiği için TÜBİTAK ULAKBİM, Yüksek Performans ve Grid Hesaplama Merkezi'ne de minnettardır.

Çıkar Çatışması: Yazarlar, çıkar çatışması olmadığını beyan etmiştir. Etik Komite Onayı: Bu çalışma için etik kurul onayı gerekmemektedir. Finansal Destek: Bu çalışma tüm yazarlar tarafından finanse edilmiştir.

Peer-review: Externally peer-reviewed.

Author Contributions: Necmettin Pirinccioglu: Concept; Design; Supervision; Resources; Analysis and Interpretation; Critical Review. Alev Arslantürk Bingul: Data Collection and Processing; Analysis and Interpretation; Literature Search; Writing Manuscript

Acknowledgements: The author (AAB) would like to thank TUBİTAK for the scholarship entitled as 2211-C National PhD Scholarship Program in

the Priority Fields in Science and Technology. Authors are also grateful to TUBİTAK ULAKBIM, High Performance and Grid Computing Center, for allowing the use of (TRUBA resources) during the molecular docking process.

Conflict of Interest: The authors have no conflicts of interest to declare. **Ethics Committee Approval:** Ethics committee approval is not required for this study.

Financial Disclosure: The authors declared that this study has received no financial support.

REFERENCES

- 1. Cui J, Li F, Shi ZL. Origin and evolution of pathogenic coronaviruses. *Nat Rev Microbiol*. 2019;17:181–192.
- 2. Malik YA. Properties of coronavirus and SARS-CoV-2. Malays. *J Pathol.* 2020;42:3–11.
- 3. Palayew A, Norgaard O, Safreed-Harmon K, Andersen TH, Rasmussen LN, Lazarus JV. Pandemic publishing poses a new COVID-19 challenge. *Nat Hum Behav.* 2020;4:666–669.
- 4. Tu YF, Chien CS, Yarmishyn AA, et al. A review of SARS-CoV-2 and the ongoing clinical trials. *Int J Mol Sci.* 2020;21:2657.
- 5. Li Q, Guan X, Wu P, et al. Early transmission dynamics in wuhan, China, of novel coronavirus—infected pneumonia. *N Engl J Med.* 2020;382:1199–1207.
- 6. Al-Aly Z, Xie Y, Bowe B. High-dimensional characterization of post-acute sequelae of COVID-19. *Nature*. 2021;594:259–264.
- 7. Zhou P, Yang XL, Wang XG, et al. A pneumonia outbreak associated with a new coronavirus of probable bat origin. *Nature*. 2020;579:270–273.
- 8. Satarker S, Nampoothiri M. Structural proteins in severe acute respiratory syndrome coronavirus-2. *Arch Med Res.* 2020;51:482–491.
- 9. Schoeman D, Fielding BC. Coronavirus envelope protein: current knowledge. *J Virol*. 2019;16:1–22.
- Artika IM, Dewantari AK, Wiyatno A. Molecular biology of coronaviruses: current knowledge. *Heliyon*. 2020;6:4743-54.
- 11. Benvenuto D, Giovanetti M, Ciccozzi A, Spoto S, Angeletti S, Ciccozzi M. The 2019-new coronavirus epidemic: evidence for virus evolution. *J Med Virol.* 2020;92:455–459.
- 12. Gao H, Dai R, Su R. Computer-aided drug design for the pain-like protease (PL^{pro}) inhibitors against SARS-CoV-2. *Biomed Pharmacother.* 2023;159:114247.
- 13. Kim H, Hauner D, Laureanti JA, Agustin K, Raugei S, Kumar N. Mechanistic investigation of SARS-CoV-2 main protease

- to accelerate design of covalent inhibitors. *Sci Rep.* 2022;12:21037.
- 14. Malone B, Urakova N, Snijder E, Campbell EA. Structure and function of the coronavirus replication-transcription complex. *Nature Reviews Microbiol.* 2022;20(3):181–194.
- Mielech AM, Kilianski A, Baez-Santos, YM, et al. MERS-CoV papain-like protease has delSGylating and deubiquitinating activities, *Virology*. 2014;450(451):64– 70
- 16. Lindner HA, Lytvyn V, Ql H, et al., Selectivity in ISG15 and ubiquitin recognition by the SARS coronavirus papain-like protease. *Arch Biochem Biophys.* 2007;466(1):8–14.
- 17. Barretto N, Jukneliene D, Ratia K, et al. The papain-like protease of severe acute respiratory syndrome coronavirus has deubiquitinating activity. *J Virol*. 2005;79(24):15189–15198.
- 18. Zhou P, Yang XL, Wang XG, et al., A pneumonia outbreak associated with a new coronavirus of probable bat origin. *Nature*. 2020;579(7798):270–273.
- Jayk Bernal A, Gomes da Silva MM, Musungaie DB, et al. Molnupiravir for Oral Treatment of Covid-19 in Nonhospitalized Patients. N Engl J Med. 2022;386:509–520.
- Eng H, Dantonio AL, Kadar EP, et al. Disposition of Nirmatrelvir, an Orally Bioavailable Inhibitor of SARS-CoV-2 3C-Like Protease, across Animals and Humans. *Drug Metab Dispos*. 2022;50:576–590.
- 21. Xia Z, Sacco M, Hu Y, et al. Rational Design of Hybrid SARSCoV-2 Main Protease Inhibitors Guided by the Superimposed Cocrystal Structures with the Peptidomimetic Inhibitors GC-376, Telaprevir, and Boceprevir. ACS Pharmacol Transl Sci. 2021;4:1408–1421.
- 22. Ma C, Sacco MD, Hurst B, et al. Boceprevir, GC-376, and calpain inhibitors II, XII inhibit SARS-CoV-2 viral replication by targeting the viral main protease. *Cell Res.* 2020;30: 678–692.
- 23. Ferreira GM, Pillaiyar T, Hirata MH, Poso A, Kronenberger T. Inhibitors induced conformational changes in SARS-COV-2 papain-like protease. *Sci Rep.* 2022;12:11585.
- 24. Thangavel N, Albratty M. Pharmacophore model-aided virtual screening combined with comparative molecular docking and molecular dynamics for identification of marine natural products as SARS-CoV-2 papain-like protease inhibitors. *Arabian J Chem.* 2022;15:1-12
- 25. Jadhav P, Huang B, Osipiuk J, et al. Structure-based design of SARS-CoV-2 papain-like protease inhibitors. *Eur J Med Chem.* 2024;264:116011.

- Dhananjay J, Selvaraj A, Vyshnavi T, et al. Virtual high throughput screening: Potential inhibitors for SARS-CoV-2 PL^{PRO} and 3CL^{PRO} proteases. *Eur J Pharma*. 2021;901:174082,
- Deepesh KP, Harish KM, Elizabeth S. Exploring the binding dynamics of covalent inhibitors within active site of PL^{pro} in SARS-CoV-2. Comp Bio Chem. 2024;12:108132.
- 28. Richards FM. Areas, volumes, packing, and protein structure. *Ann Rev Biophys Bioeng*. 1977;6:151–176.
- 29. Connolly ML. Solvent-accessible surfaces of proteins and nucleic acids. Dissertation. University of California, Berkeley; 1981.
- 30. Kuntz ID, Blaney JM, Oatley SJ, Langridge R, Ferrin TE. A geometric approach to macromolecule-ligand interactions. *J Mol Biol.* 1982;161(2):269–288.
- 31. Ashouri M, Firouzi R. Virtual Screening and Binding Mode Analysis of Selected FDA Approved Drugs Against PL^{pro} Target: An Effort to Identify Therapeutics to Combat COVID-19. *Med Discoveries*. 2023;2(9):1070.
- 32. Garland O, Ton AT, Moradi S, et al. Large-scale virtual screening for the discovery of SARS-CoV-2 papain-like protease (PLpro) non-covalent inhibitors. *J Chem Inform Model*. 2023;63(7):2158–2169.